

m7GHub V2.0: an updated database for decoding the N7-methylguanosine (m⁷G) epitranscriptome

Wang, Xuan; Zhang, Yuxin; Chen, Kunqi; Liang, Zhanmin; Ma, Jiongming; Xia, Rong; de Magalhães, João Pedro; Rigden, Daniel J; Meng, Jia; Song, Bowen

DOI:

[10.1093/nar/gkad789](https://doi.org/10.1093/nar/gkad789)

License:

Creative Commons: Attribution (CC BY)

Document Version

Publisher's PDF, also known as Version of record

Citation for published version (Harvard):

Wang, X, Zhang, Y, Chen, K, Liang, Z, Ma, J, Xia, R, de Magalhães, JP, Rigden, DJ, Meng, J & Song, B 2024, 'm7GHub V2.0: an updated database for decoding the N7-methylguanosine (m⁷G) epitranscriptome', *Nucleic Acids Research*, vol. 52, no. D1, pp. D203-D212. <https://doi.org/10.1093/nar/gkad789>

[Link to publication on Research at Birmingham portal](#)

General rights

Unless a licence is specified above, all rights (including copyright and moral rights) in this document are retained by the authors and/or the copyright holders. The express permission of the copyright holder must be obtained for any use of this material other than for purposes permitted by law.

- Users may freely distribute the URL that is used to identify this publication.
- Users may download and/or print one copy of the publication from the University of Birmingham research portal for the purpose of private study or non-commercial research.
- User may use extracts from the document in line with the concept of 'fair dealing' under the Copyright, Designs and Patents Act 1988 (?)
- Users may not further distribute the material nor use it for the purposes of commercial gain.

Where a licence is displayed above, please note the terms and conditions of the licence govern your use of this document.

When citing, please reference the published version.

Take down policy

While the University of Birmingham exercises care and attention in making items available there are rare occasions when an item has been uploaded in error or has been deemed to be commercially or otherwise sensitive.

If you believe that this is the case for this document, please contact UBIRA@lists.bham.ac.uk providing details and we will remove access to the work immediately and investigate.

m7GHub V2.0: an updated database for decoding the N7-methylguanosine (m⁷G) epitranscriptome

Xuan Wang^{1,2,†}, Yuxin Zhang^{2,3,†}, Kunqi Chen^{4,†}, Zhanmin Liang², Jiongming Ma^{2,3}, Rong Xia⁵, João Pedro de Magalhães⁶, Daniel J. Rigden³, Jia Meng^{2,3,7} and Bowen Song^{1,*}

¹Department of Public Health, School of Medicine & Holistic Integrative Medicine, Nanjing University of Chinese Medicine, Nanjing 210023, China

²Department of Biological Sciences, Xi'an Jiaotong-Liverpool University, Suzhou, 215123, China

³Institute of Systems, Molecular and Integrative Biology, University of Liverpool, L7 8TX, Liverpool, UK

⁴Key Laboratory of Ministry of Education for Gastrointestinal Cancer, School of Basic Medical Sciences, Fujian Medical University, Fuzhou 350004, China

⁵Department of Financial and Actuarial Mathematics, Xi'an Jiaotong-Liverpool University, Suzhou, 215123, China

⁶Institute of Inflammation and Ageing, University of Birmingham, B15 2WB, Birmingham, UK

⁷AI University Research Centre, Xi'an Jiaotong-Liverpool University, Suzhou 215123, China

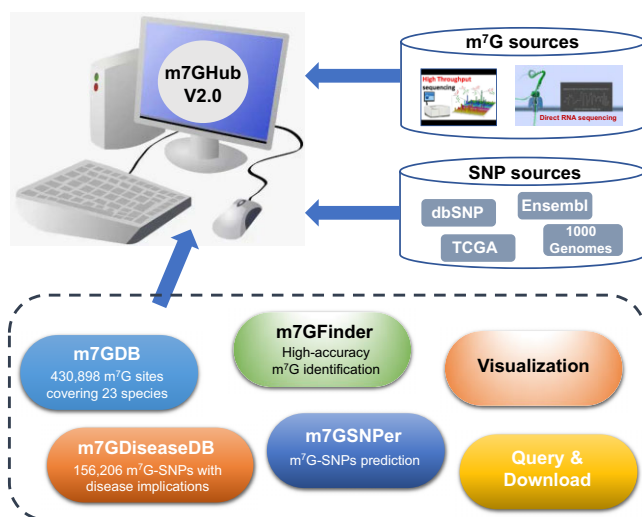
*To whom correspondence should be addressed. Bowen Song. Email: bowen.song@njucm.edu.cn

†Contributed equally to this work.

Abstract

With recent progress in mapping N7-methylguanosine (m⁷G) RNA methylation sites, tens of thousands of experimentally validated m⁷G sites have been discovered in various species, shedding light on the significant role of m⁷G modification in regulating numerous biological processes including disease pathogenesis. An integrated resource that enables the sharing, annotation and customized analysis of m⁷G data will greatly facilitate m⁷G studies under various physiological contexts. We previously developed the m7GHub database to host mRNA m⁷G sites identified in the human transcriptome. Here, we present m7GHub v.2.0, an updated resource for a comprehensive collection of m⁷G modifications in various types of RNA across multiple species: an m7GDB database containing 430 898 putative m⁷G sites identified in 23 species, collected from both widely applied next-generation sequencing (NGS) and the emerging Oxford Nanopore direct RNA sequencing (ONT) techniques; an m7GDiseaseDB hosting 156 206 m⁷G-associated variants (involving addition or removal of an m⁷G site), including 3238 disease-relevant m⁷G-SNPs that may function through epitranscriptome disturbance; and two enhanced analysis modules to perform interactive analyses on the collections of m⁷G sites (m7GFinder) and functional variants (m7GSNPer). We expect that m7Ghub v.2.0 should serve as a valuable centralized resource for studying m⁷G modification. It is freely accessible at: www.nmand.org/m7GHub2.

Graphical abstract



Received: July 17, 2023. Revised: August 18, 2023. Editorial Decision: September 13, 2023. Accepted: September 18, 2023

© The Author(s) 2023. Published by Oxford University Press on behalf of Nucleic Acids Research.

This is an Open Access article distributed under the terms of the Creative Commons Attribution License (<http://creativecommons.org/licenses/by/4.0/>), which permits unrestricted reuse, distribution, and reproduction in any medium, provided the original work is properly cited.

Introduction

Over 170 types of chemical modification are naturally decorated on cellular RNAs of all three kingdoms of life, modulating various biological processes such as translation, RNA stability and RNA metabolism (1,2). Among them, N7-methylguanosine (m⁷G) is the most ubiquitous RNA cap modification added to the 5' cap at the initial stage of transcription (3). Recent studies suggested that m⁷G capping modulates nearly the entire life cycle of messenger RNA (mRNA), including mRNA splicing (4), translation (5), RNA processing and metabolism (6) and transcription (7), and influences various cellular processes including gene expression and transcript stabilization (8). Additionally, the presence of m⁷G modification in ribosomal RNA (rRNA) (9) and transfer RNA (tRNA) (10) has also been reported, and mutations that impair tRNA m⁷G methylation found to cause microcephalic primordial dwarfism (11).

We previously developed an integrated resource m7GHub to share data on m⁷G RNA modification in the human transcriptome (12). In the first release, m7GHub collected 44 058 experimentally validated human mRNA m⁷G sites and 57 769 m⁷G-associated variants, respectively. Additionally, 1218 m⁷G disease-relevant m⁷G-SNPs were further annotated, with implications for the potential pathogenesis of ~600 disease phenotypes.

To date, several high-throughput sequencing techniques have been developed and applied for transcriptome-wide profiling of m⁷G RNA modification. The m⁷G-MeRIP-seq was first introduced in 2019 to profile m⁷G distribution in human and mouse transcriptome, respectively (13). This antibody-based immunoprecipitation technique reveals m⁷G-containing regions with a resolution ~100 bp and has since been further applied to multiple species including rat and zebra fish (14–16). By combining the conventional MeRIP-seq approach with ultraviolet cross-linking, m⁷G-miCLIP-seq achieved an improved resolution of ~30 bp (17). In addition, base-resolution approaches such as m⁷G-seq (13) and m⁷G-MaP-seq (18) offer the precise location of m⁷G modification sites. Several overall patterns of m⁷G modification sites have also been reported across profiling techniques. Specifically, statistically significant GA- or GG-enriched motifs were identified in peaks using m7G-MeRIP-seq (13), while AG-rich contexts were reported from m7G-miCLIP-seq (17). Additionally, diverse sequence motifs around base-resolution m⁷G sites have also been reported by m7G-seq, with G(m⁷G)A and A(m⁷G)A ranking the top two motifs. Taken together, these findings suggested that additional methyltransferase(s) may be involved for m⁷G installation (13). Besides next-generation sequencing (NGS)-based methods, the newly emerged direct RNA sequencing platform developed by Oxford Nanopore Technology (ONT) also provides a promising alternative, allowing the simultaneous real-time identification of any natural modifications in the RNA molecule based on characteristic signals (19). Several pilot studies have offered specific or mixed identification of modified residues, such as m6Anet (m⁶A) (20), MINES (m⁶A) (21), nanoPsu (pseudouridine) (22), ELIGOS (mixed) (23) and Tombo (mixed). The ELIGOS and Tombo studies report a set of putative modified residues without differentiating the modification type, but these unknown types of candidate modification site can be further labeled using deep learning models.

In response to our rapidly expanding knowledge in RNA modification, bioinformatics databases have been developed to share, annotate and interpret the generated datasets. These bioinformatics efforts include: MODOMICS for querying RNA modification pathways (24); RMBase v.2.0 to collect of RNA modification sites (25); RMVar for unveiling RNA modification (RM)-associated variants (26); RM2Target for collection of writers, erasers and readers (WERs) of RNA modifications (27); m6A-Atlas as an m⁶A knowledgebase (28) and ConsRM for quantifying m⁶A conservation (29). However, to the best of our knowledge, resources for m⁷G-related knowledge are still limited to m7GHub.

In this study, we have upgraded m7GHub to version 2.0 by integrating all recently identified m⁷G RNA modification sites derived from NGS and ONT-based studies, from which m⁷G-affecting variants were revealed using a deep learning model. The m7GHub v.2.0 consists of the following major updates: (i) m7GDB: a comprehensive m⁷G database consisting of 258 206 NGS-based m⁷G sites and the first collection of 172 692 putative m⁷G sites derived from ONT samples with rich functional annotations, covering a total of 23 species. (ii) m7GDiseaseDB: a database holding the most complete collection of 156 206 m⁷G-associated variants that may add or remove an m⁷G methylation site, with 3238 disease-relevant variants that may shed light on disease mechanisms acting through epitranscriptome layer circuitry. (iii) Enhanced modules allow interactive analysis of the database collections and user-uploaded datasets, from which putative m⁷G sites (m7GFinder) and epitranscriptome disturbance (m7GSNPer) of user-interested genome regions/genetic variants can be determined. The overall design of m7GHub v.2.0 is outlined in Figure 1. We expect that m7GHub v.2.0 will be a valuable one-stop platform for researchers who are interested in m⁷G modification: it is freely accessible at: www.rnamd.org/m7GHub2.

Materials and methods

Collection of m⁷G sites based on profiling techniques

The m⁷G sites collected in m7GHub v.2.0 were derived from both high-throughput sequencing (NGS) and Oxford Nanopore direct RNA sequencing (ONT) samples. Regarding NGS-based studies, the m⁷G sites were obtained from 74 sequencing samples using five different m⁷G profiling techniques. Additionally, 116 direct RNA sequencing samples, comprising 42 FAST5 and 74 FASTQ files, were collected from 37 independent studies in the NCBI GEO database (Supplementary Tables S1 and S2). Specifically, the collected m⁷G sites were classified into three different groups as illustrated next:

- i. **NGS techniques (base-resolution):** the m⁷G sites classified in this group were extracted from NGS-based studies at base-resolution level. The genome coordinates of m⁷G residues were extracted from the relating GSE or corresponding supplementary files of m7G-seq and m7G-MaP-seq studies, respectively. For m7G-seq, we re-processed the raw sequencing data to map the base-resolution m⁷G sites to human genome assembly hg38, following the same protocol implemented in the original study (13).
- ii. **NGS techniques (m⁷G-containing region):** the m⁷G-containing regions were extracted from m7G-MeRIP-

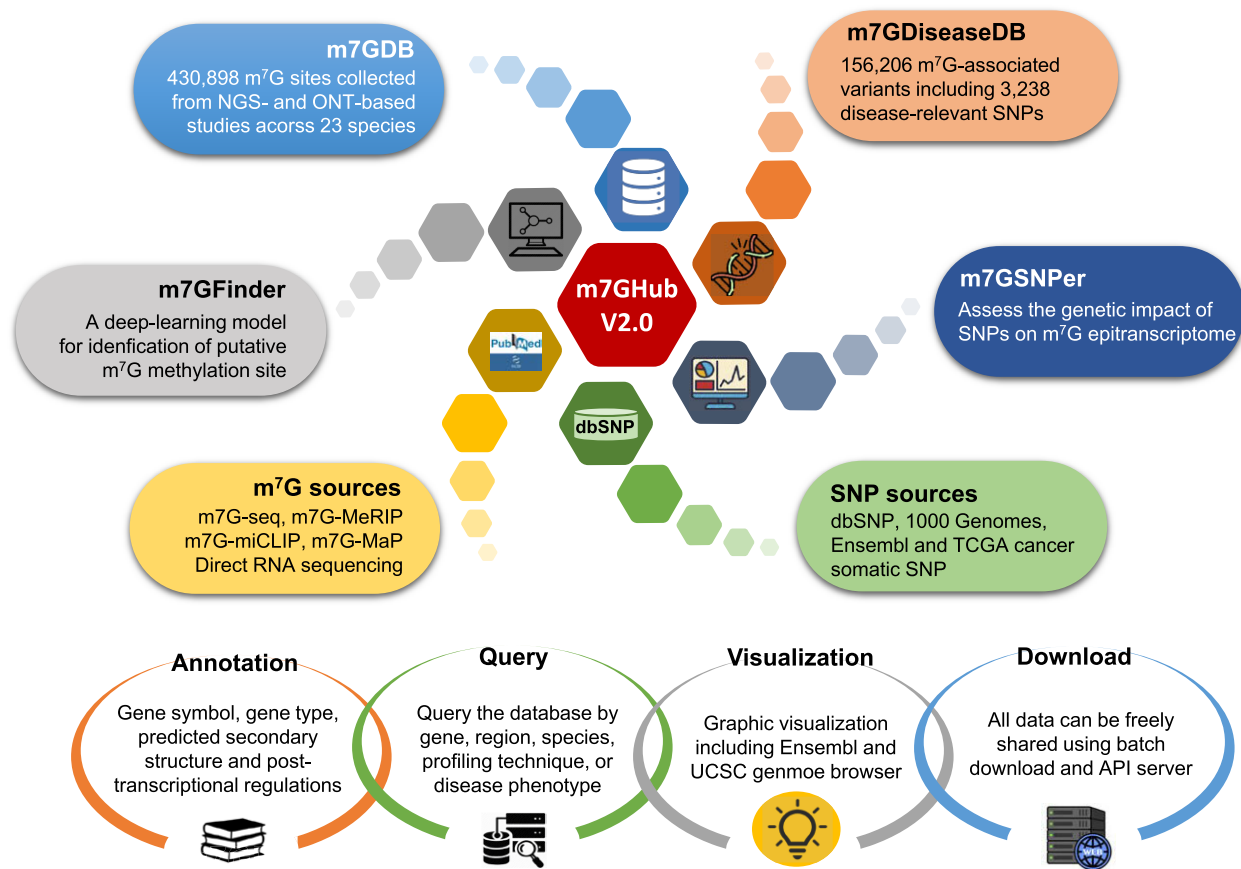


Figure 1. The overall construction of m7GHub v2.0. The updated m7GHub v2.0 consists of four major components: (i) m7GDB: the first m⁷G database containing ~430 000 putative m⁷G sites collected from both NGS- and ONT-derived samples; (ii) m7GFinder: a deep learning-based high accuracy m⁷G predictor covering m⁷G identification in four different species; (iii) m7GSNPer: a real-time analysis module to assess the impact of genetic variants on database collection; (iv) m7GDiseaseDB: a database holding ~150 000 functional variants involved in m⁷G modification, with implications for the potential pathogenesis of ~1300 known phenotypes. An integrated web interface offers query, search, visualize and download function of all collected data is freely accessible at: www.namd.org/m7GHub2.

seq (~150 bp) and m⁷G-miCLIP-seq (~30 bp), respectively. Specifically, the m⁷G-containing regions from m⁷G-MeRIP-seq were obtained using a common pipeline. The raw FASTQ datasets were directly downloaded from NCBI Gene Expression Omnibus (GEO) (30), the raw reads were trimmed and aligned to the reference genome using HISAT2 (31), and peak-calling process was implemented by exomePeak2 (32). Besides m⁷G-MeRIP-seq, the genome coordinates of m⁷G-containing regions from m⁷G-miCLIP-seq were extracted from the supplementary files of its original study (17).

- iii. **ONT-derived and deep-learning prediction:** to try to unveil the landscape of m⁷G methylation generated by direct RNA sequencing techniques, we obtain the ONT-based m⁷G sites by large-scale prediction of modified guanosines using our previously developed deep neural network models (33). As no tools were available for specifically predicting m⁷G sites from direct RNA sequencing data, the Tombo and ELIGOS were used to screen out all non-canonical guanosines from direct RNA sequencing samples. Specifically, the raw FAST5 data were re-squiggled with the ‘Tombo re-squiggle’ module and candidate modification sites were detected

by the ‘Tombo de novo modification detection’ module based on signal shifts. ELIGOS used the base calling errors (i.e. insertion, deletion, substitution and decreased base call qualities) caused by the presence of non-canonical bases. Raw FAST5 data were base called with Guppy and aligned to their reference genome with Minimap2. Then, ELIGOS extracted the base call error profile from the alignment SAM file and compared it with expected one. Sites with significantly higher errors were reported as potential modification sites. Consequently, Tombo and ELIGOS reported a set of putative modified guanosines without differentiating their modification type. The modified guanosines were further assessed by our previously developed neural network (33), trained on the NGS-validated m⁷G sites from four species (human, mouse, rat and zebra fish), respectively. Only the modified guanosines passing a strict cut-off (average prediction score >0.5 and upper bound of *P*-value < 0.05) were retained as putative m⁷G sites and included in the m7GDB database.

Evaluating the epitranscriptome impact of genetic variants on m⁷G methylation status

In this study, two types of genetic variant were considered to assess their epitranscriptome impact on m⁷G methylation status. The germline variants were extracted from dbSNP (v151) (34), 1000 Genomes (Phase 3 Mitochondrial Chromosome Variants set) and Ensembl 2022 (Ensembl release 106) (35). In addition, 33 different cancer types of human somatic variants were collected from the Cancer Genome Atlas (TCGA) (release v.35) (36). Together, a total of 6 0826 918 germline variants and 2 264 915 somatic variants identified in four species were included, and the detailed datasets of genetic variants analyzed in this study can be found in Supplementary Table S3.

Following the well-defined definition for predicting m⁷G-affecting variants in m⁷GHub and other related studies (26,37), an m⁷G-associated variant was characterized based on its ability to cause the gain or loss of an m⁷G modification site, as predicted by our previously described deep neural network models (33). Three different confidence levels were further defined: (i) high: a genetic variant directly altered an experimentally validated m⁷G site at base-resolution level (m⁷G-seq or m⁷G-MaP-seq), leading to the loss of the modified nucleotide; (ii) medium: a genetic variant altered a nucleotide within the 41-nt flanking window of a base-resolution m⁷G site or within an m⁷G-containing region (~30–150 nt, identified by m⁷G-MeRIP-seq or m⁷G-miCLIP-seq), resulting in the loss of an m⁷G status in the mutated sequence, as determined by the deep learning model and (iii) low: the low confidence level covers the transcriptome-wide prediction for reference- and mutated-sequence (altered by a genetic variant) around guanines, the significant decrease or increase in the m⁷G probability were reported by the deep learning model to define m⁷G-loss or m⁷G-gain mutation, respectively. Specifically, we calculated the association level (AL) between genetic variant and m⁷G site as follows:

$$AL = \begin{cases} 2P_{SNP} - 2 \max(0.5, P_{WT}) & \text{for gain} \\ 2P_{WT} - 2 \max(0.5, P_{SNP}) & \text{for loss} \end{cases} \quad (1)$$

Where the association level (AL) was calculated based on the probability of m⁷G methylation status for reference (wide type, P_{WT}) and mutated sequence (SNP altered, P_{SNP}) ranging from 0 to 1, with a value of 1 indicating the greatest epitranscriptome impact of the genetic variants on m⁷G status. The statistical significance was assessed by comparison to the ALs of all genetic variants, from which we use the upper bound of the P -value to represent the absolute ranking of each m⁷G-associated variant. Only the variants with a P -value < 0.05 (within the top 5% ALs of all genetic variants) were retained in the database collection.

Functional annotation for m⁷G sites and m⁷G-associated variants

Functional annotations were integrated to help better interpret the regulatory roles of the m⁷G epitranscriptome. The collected m⁷G sites and functional variants were first annotated with basic information such as gene annotation, transcript structure and predicted RNA secondary structure information (38). The potential involvement of post-transcriptional regulations was addressed with data collected from POSTAR2 (39) (RBP binding regions), miRanda (40) and startBase2 (41) (miRNA–RNA interaction), and UCSC

Table 1. Collection of m⁷G sites in m⁷GDB

Species	Experimentally validated NGS techniques		ONT-derived and deep-learning prediction	Total
	1bp	~30–300 bp	1bp	
Human	8402	161 316	76 077	245 795
Mouse	/	18 595	13 828	32 423
Rat	/	49 440	/	49 440
Zebra fish	/	20 342	/	20 342
19 other species	111	/	82 787	82 898
Total	8513	249 693	172 692	430 898

browser (42) annotation (GT-AG splicing sites). In addition, the m⁷G-associated variants were annotated with mutation type (nonsynonymous or synonymous variant), TCGA barcode, RS ID, deleterious level (predicted by five independent scores (43–46)). This information was derived from the ANNOVAR package (47), dbSNP (34) and the TCGA database (36).

Potential involvement of m⁷G methylation in disease pathogenesis

A large number of disease-related variants (TagSNPs) were obtained from ClinVar (48), the GWAS catalog (49) and Johnson and O'Donnell's database (50). In addition, the TagSNPs were used to implement linkage disequilibrium (LD) analysis using PLINK (51) tool (parameters: $-r2$ $-ld$ -snp-list $-ld$ -window-kb 1000 $-ld$ -window 10 $-ld$ -window-r2 0.8). The disease TagSNPs and their LD mutations were mapped to all m⁷G-associated variants to explore the potential pathogenesis of known disease-phenotypes through m⁷G regulation.

Database and web interface implementation

Hyper text markup language (HTML), cascading style sheets (CSS) and hypertext preprocessor (PHP) were used in the fundamental development of m⁷GHub v.2.0 web interfaces. We implemented MySQL and ECharts to present metadata and statistical diagrams, respectively. Additionally, the interactive exploration of user-interested genome coordinates were visualized by JBrowse genome browser (52).

Results

m⁷G sites collected in m⁷GDB

The updated m⁷GDB database holds a total of 430 898 m⁷G sites (see Table 1) collected from NGS- and ONT-based studies, representing a significant expansion in both number of collected m⁷G sites (~10-fold expansion) and covered species (from human only to 23 species) compared to the first release. Specifically, the NGS-derived m⁷G sites cover seven species including human (169 718), mouse (18 595), rat (49 440), zebra fish (20 342), yeast (88), *Arabidopsis* (19) and *Escherichia coli* (4). For the human collection, the m⁷G sites were further classified according to their profiling techniques, including base-resolution level (8402 sites, m⁷G-seq and m⁷G-MaP-seq) and m⁷G-containing region (22 783 sites, m⁷G-miCLIP-seq, ~30 bp; 138 534 sites, m⁷G-MeRIP-seq, ~150 bp). For datasets collected from direct RNA sequencing studies, a total of 172 692 modified guanines annotated with m⁷G proba-

Table 2. Comparison of m7GHub v2.0 with other epitranscriptome databases

	m7GHub v.2.0	m7GHub v1.0 (12)	RMDisease v.2.0 (37)	RMVar (26)	RMBase v2.0 (25)	DirectRM DB (53)
Number of m ⁷ G sites collected	430 898	44 058	9365	43 367	318	1189
Covered species (m ⁷ G site)	23	1	1	2	3	1
Number of m ⁷ G-associated SNP	156 206	57 769	24 049	64 867	7	/
Covered species (m ⁷ G-SNP)	4	1	1	2	1	/
Disease-associated m ⁷ G-SNP	3238	1218	507	861	/	/
Interactive analyses (m ⁷ G site identification)	Yes (4 species)	1	/	/	/	/
Interactive analyses (m ⁷ G-SNP identification)	Yes (4 species)	1	1	/	/	/

Table 3. m⁷G-associated variants collected in m7GDiseaseDB

Species	Confidence level	m ⁷ G-associated variants			ClinVar			GWAS		
		Loss	Gain	Total	SNP	Disease	Gene	SNP	Disease	Gene
Human (Germline SNP)	High	1316	/	1316	94	92	90	24	22	24
	Medium	9699	/	9699	660	361	413	107	73	97
	Low	7518	14 608	22 126	840	515	581	256	141	240
Human (Somatic SNP)	High	4018	/	4018	92	113	83	5	5	5
	Medium	30 073	/	30 073	569	309	322	53	41	48
	Low	7911	22 264	30 175	538	349	393	53	41	51
Mouse	High	530	/	530	/	/	/	/	/	/
	Medium	4055	/	4055	/	/	/	/	/	/
	Low	7595	11 384	18 979	/	/	/	/	/	/
Rat	Medium	4225	/	4225	/	/	/	/	/	/
	Low	1694	1503	3197	/	/	/	/	/	/
Zebra fish	Medium	7285	/	7285	/	/	/	/	/	/
	Low	10 647	9881	20 528	/	/	/	/	/	/

Note: The TCGA somatic variants were extracted from 33 different types of human cancer projects. The m⁷G-associated variants classified into high confidence level refer to mutations directly destroying base-resolution modified nucleotides (m⁷G site). The numbers in the ‘ClinVar’ and ‘GWAS’ sections represent the number of m⁷G-associated variants mapped to the disease-related TagSNPs having ClinVar or GWAS records, respectively.

bility were collected across 21 species at base-resolution level, such as human (76 077), mouse (13 828), fruit fly (298), pig (366), maize (8939) and *Arabidopsis* (3083). In particular, the m⁷G epitranscriptome in 20 species is covered for the first time, and data from direct RNA sequencing samples included. Compared to the previous version and other epitranscriptomic databases (RMBase (25), RMVar (26) and RMDisease (37)), m7GHub represents the most comprehensive knowledgebase for collections of m⁷G methylation so far (Table 2).

Potential disease pathogenesis involving m⁷G disturbance (m7GDiseaseDB)

m7GDiseaseDB holds a total of 156 206 genetic variants that may add or remove m⁷G methylation status in four species (Table 3), including human (97 407), mouse (23 564), rat (7422) and zebra fish (27 813), providing the most comprehensive map of genetic factors potentially relating to m⁷G disturbance so far. To unveil the potential mechanisms of disease phenotypes functioning at the epitranscriptome layer, we then mapped all collected human m⁷G-associated variants to pathogenic TagSNPs and their LD mutations. We found that 3238 m⁷G-associated variants localized on 1651 genes were recorded with 1308 known disease phenotypes, which is nearly three times the number in the previous version. Additionally, 64 266 m⁷G-associated variants were also derived from TCGA cancer somatic mutations, revealing the potential

involvement of m⁷G methylation in 33 types of human cancer. Finally, we identified the disease phenotypes and TCGA cancer types that are most strongly linked with m⁷G disturbance (Supplementary Table S4).

Enhanced web interface and usage

The web interface of m7GHub v2.0 has been re-designed to present an informative, fast and user-friendly one-stop knowledgebase for m⁷G study, which enables users to quickly query, carry out customized searches of and freely download all collected datasets. Four major modules were presented in m7GHub, namely m7GDB, m7GDiseaseDB, m7GFinder and m7GSNPer.

m7GDB

The experimentally validated m⁷G sites were collected in m7GDB module. Users can visualize the landscape of m⁷G modification in different species according to the profiling techniques (Figure 2A). For example, users can query the deposited m⁷G-containing region by clicking the ‘NGS (m⁷G region)’ button on the top menu bar, the returned page first summarizes the statistical distribution of collected m⁷G region categorized by species, profiling technique, tissue/cell line and gene type (Figure 2B). Various filters allow users to further filter their data of interest, including gene type and involvement of post-transcriptional regulation (Figure 2C). In addition, a position bar offers a function to extract customized regions

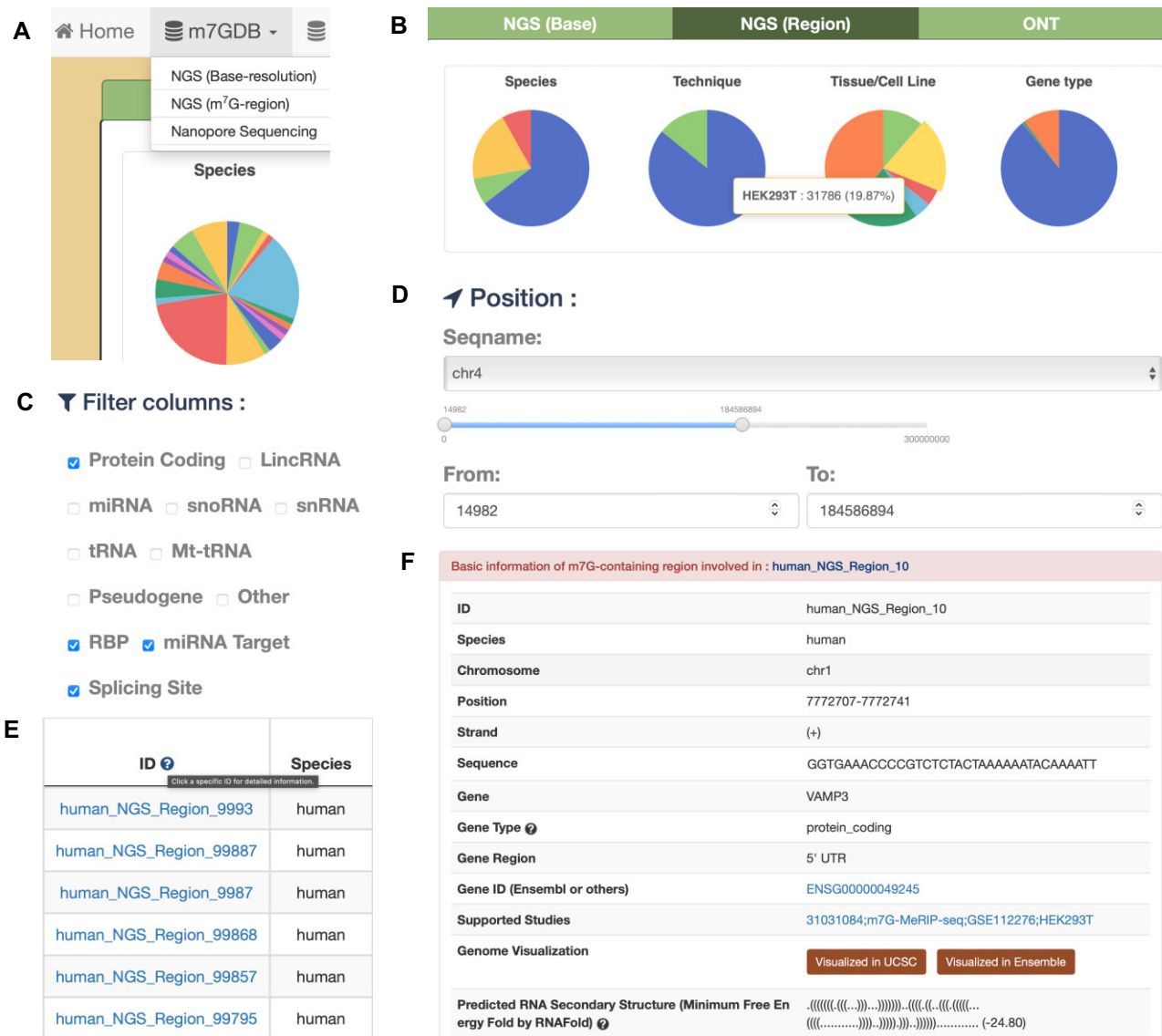


Figure 2. Contents of m7GDB. (**A** and **B**) The m⁷G sites collected in m7GDB were classified into three different group according to their profiling techniques; users can briefly check the statistical distribution of collected data summarized by pie charts. (**C** and **D**) Several options were provided to further filter the datasets, including a position par to extract specific genomic region of interests. (**E** and **F**) Once customized filtering has been applied, the user can click the site ID to view the detailed information of a specific m⁷G site.

of user interest (Figure 2D). The returned results exclusively display m⁷G sites that satisfy all selected filter options (Figure 2E): users can simply click on the site ID to access detailed information about a specific m⁷G site (Figure 2F).

m7GDiseaseDB

The m⁷G-associated variants and disease associations were collected in m7GDiseaseDB (Figure 3), from which users can query each m⁷G-associated SNP with detailed annotations such as reference sequence, mutated sequence, relative position of SNP, potential involvement in post-transcriptional regulation (miRNA targets, RBP binding, splicing events), crosslinks to dbSNP/GtRNAdb and their epitranscriptome effects on m⁷G status (gain or loss function). The disease associations can be obtained by clicking 'GWAS' or 'ClinVar' buttons from the filter columns. In addition, the 'Disease' option on the search box allows users to query all m⁷G-associated variants linking to a specific disease pheno-

type, along with other search options such as gene symbol, genome coordinate and RS ID. Finally, the m7GDiseaseDB also offers various graphic visualizations that displaying the position of the m⁷G-SNPs along the gene and genomic regions of interest, such as Ensembl and UCSC genome browser.

Analysis modules (m7GFinder and m7GSNPer)

To allow users to perform interactive analyses on the collected datasets, two enhanced modules are presented based on our previously developed deep neural network models (33). The m7GFinder was developed for high-accuracy prediction of putative m⁷G sites from user-uploaded RNA sequences (standard FASTA format). A minimum sequence length of 41 nt is required as input data (Figure 4A). The multi-instance learning framework treats each entire input sequence as a 'bag' and reports its bag-level label (m⁷G probability). Importantly, the m7GFinder reports the prediction label at the bag level (the entire input sequence), rather than a specific nucleotide (Figure 4B). Consequently, each input sequence with a length around

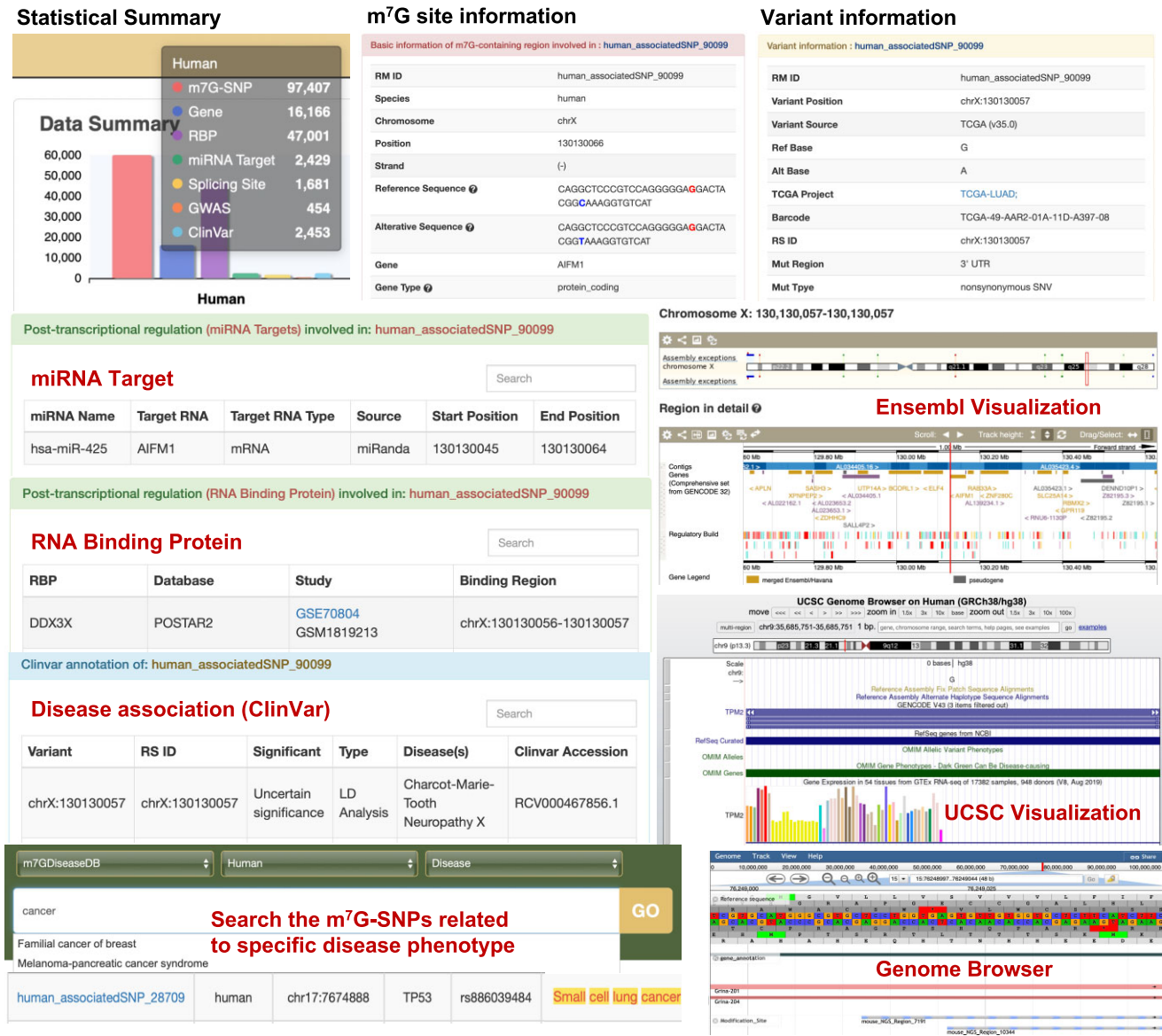


Figure 3. Enhanced web interface of m7G-DiseaseDB. User can query the collected m7G-SNPs by selecting a species and check the summary table. Users can further click the individual RM ID to access the basic information of the associated m7G-SNP and involved m7G site. The web-interface also features various graphic visualizations including Ensembl and UCSC genome browser, especially useful for presentation of SNP information. In addition, the disease associations involved m7G methylation can be extracted by searching a specific disease or phenotype.

150 nt (typical length of most m7G peaks from MeRIP-seq) is recommended. Besides m7G-Finder, the m7G-SNP module allows users to evaluate the associations between SNPs of their interest and the m7G epitranscriptome of a specific species. The standard VCF file containing a group of genetic variants is acceptable as input data for m7G-SNP, with the association level (AL) was calculated between reference and mutated sequences. The returned results of m7G-SNP can be freely downloaded with detailed column explanations (Figure 4C).

Batch download and API server

Two downloading options are provided for all datasets collected in m7G-Hub v.2.0. (i) Multiple datasets can be simultaneously selected for batch downloading on the ‘Download’ page. (ii) The application program interface (API) server pro-

vides a highly flexible download option: instructions and examples to access the API server are provided on ‘API’ page.

Discussion

With the rapid accumulation of sequencing samples derived from NGS and ONT technologies, comprehensive maps of m7G modifications under various biological contexts have been revealed. We have updated m7G-Hub to version 2.0, an all-in-one online platform designed to effectively store, annotate, analyze and share the m7G data. Compared to the first release (m7G-Hub v1.0) and other epitranscriptome databases, our updated version covered so far the most comprehensive collections of m7G-related data (please refer to Table 2), including: (i) a comprehensive database (m7GDB) of 430 898 previously reported m7G sites, including the first collection of putative m7G sites from ONT-derived samples,

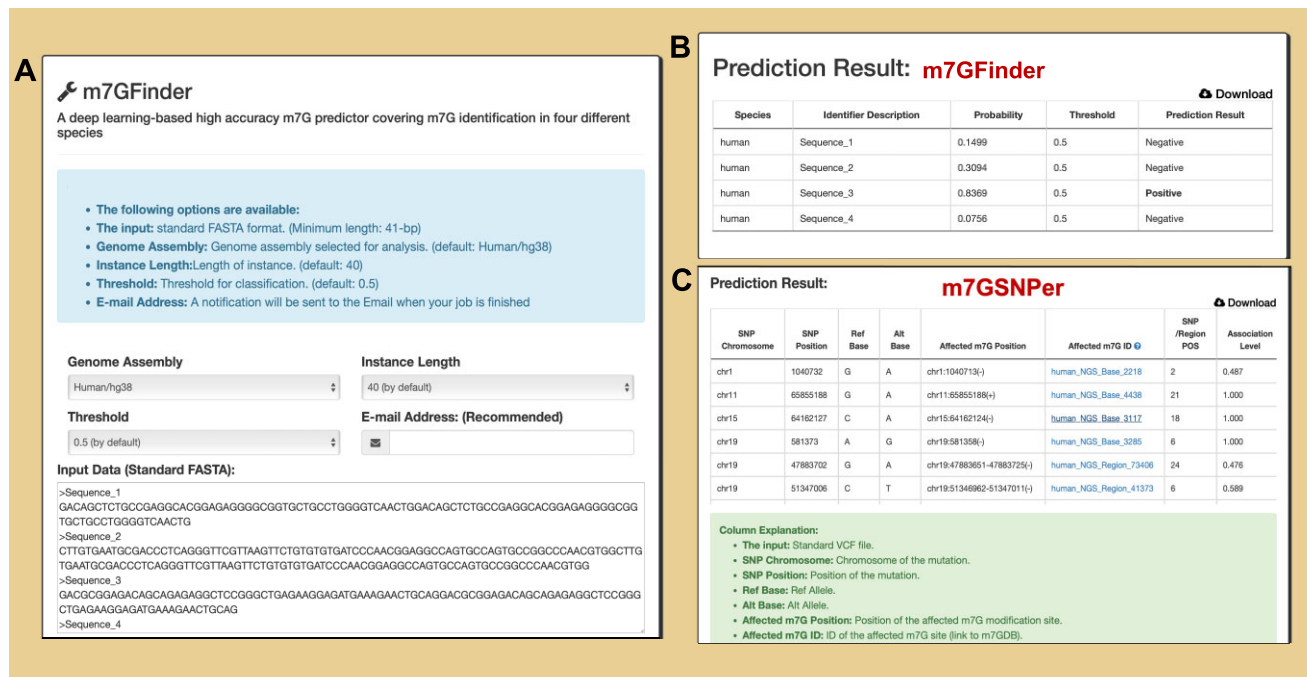


Figure 4. Contents of m7GFinder and m7GSNPer. **(A)** Web interface of m7GFinder. **(B)** Prediction results from m7GFinder. The m7GFinder reports the prediction label at the bag level (the entire input sequence), rather than a specific nucleotide. **(C)** Prediction results from m7GSNPer. The explanation for each column has been presented clearly, and the data is available for free download and sharing.

marking an 10-fold expansion compared with the first release. (ii) m⁷G-associated variants identified in four species, of which potential involvement in 1308 disease phenotypes was revealed for 3238 disease-related m⁷G-affecting SNPs (m7GDiseaseDB). In addition, two deep learning-based analysis tools (m7GFinder and m7GSNPer) were developed to support analyses of the database or user-uploaded data.

In conclusion, m7GHub v.2.0 offers an extensive repository of m⁷G epitranscriptome data across various species. However, in the current version, the landscape of putative m⁷G modification from direct RNA sequencing samples was predicted by deep-learning model of modified guanines, and thus only offers limited reliability. With the rapid advancement and widespread adoption of direct RNA sequencing techniques, we can expect the development of software to directly identify m⁷G modifications from direct RNA sequencing samples in the near future. Additionally, due to variations in the number of sequencing samples across different species, the m⁷G sites currently collected in the database cannot directly represent the overall distribution of m⁷G modification in a given species, especially for species with extremely limited sequencing samples available (e.g. yeast and *E. coli*). Consequently, the database will undergo regular updates by continuously incorporating the latest sequencing data and methodologies to ensure it remains a useful resource for the m⁷G research community.

Data availability

The raw data used to develop m7GHub v.2.0 is already publicly available in the NCBI GEO database, The Cancer Genome Atlas (TCGA release v.35), dbSNP (v.151), 1000 Genome and Ensembl 2022 (Ensembl release 106). The detailed description (accession number) can be found in Supple-

mentary Tables S1–S3. All data collected in m7GHub v.2.0 is freely accessible at: www.rnamd.org/m7GHub2.

Supplementary data

Supplementary Data are available at NAR Online.

Acknowledgements

Author contributions: B.S. conceived the idea and initialized the project; B.S., Y.Z., K.C. and Z.L. processed the m7G sequencing data; X.W. developed the prediction model and performed the SNP analysis; X.W. and R.X. developed the web-interfaces; B.S. drafted the manuscript; B.S., J.M., J.P.M. and D.J.R. revised the manuscript; All authors read and approved the final manuscript.

Funding

National Natural Science Foundation of China [32100519 and 31671373]; XJTU Key Program Special Fund [KSF-E-51 and KSF-P-02]. Scientific Research Foundation of Nanjing University of Chinese Medicine (Grant No. 013038030001). This work is supported by the Supercomputing Platform of Xi'an Jiaotong-Liverpool University.

Conflict of interest statement

None declared.

References

- Jaffrey, S.R. (2014) An expanding universe of mRNA modifications. *Nat. Struct. Mol. Biol.*, **21**, 945–946.

2. Zaccara, S., Ries, R.J. and Jaffrey, S.R. (2019) Reading, writing and erasing mRNA methylation. *Nat. Rev. Mol. Cell Biol.*, **20**, 608–624.
3. Cowling, V.H. (2009) Regulation of mRNA cap methylation. *Biochem. J.*, **425**, 295–302.
4. Konarska, M.M., Padgett, R.A. and Sharp, P.A. (1984) Recognition of cap structure in splicing in vitro of mRNA precursors. *Cell*, **38**, 731–736.
5. Muthukrishnan, S., Both, G.W., Furuichi, Y. and Shatkin, A.J. (1975) 5'-Terminal 7-methylguanosine in eukaryotic mRNA is required for translation. *Nature*, **255**, 33–37.
6. Lewis, J.D. and Izaurralde, E. (1997) The role of the cap structure in RNA processing and nuclear export. *Eur. J. Biochem.*, **247**, 461–469.
7. Pei, Y. and Shuman, S. (2002) Interactions between fission yeast mRNA capping enzymes and elongation factor Spt5. *J. Biol. Chem.*, **277**, 19639–19648.
8. Furuichi, Y., LaFiandra, A. and Shatkin, A.J. (1977) 5'-Terminal structure and mRNA stability. *Nature*, **266**, 235–239.
9. Sloan, K.E., Warda, A.S., Sharma, S., Entian, K.D., Lafontaine, D.L.J. and Bohnsack, M.T. (2017) Tuning the ribosome: the influence of rRNA modification on eukaryotic ribosome biogenesis and function. *RNA Biol.*, **14**, 1138–1152.
10. Guy, M.P. and Phizicky, E.M. (2014) Two-subunit enzymes involved in eukaryotic post-transcriptional tRNA modification. *RNA Biol.*, **11**, 1608–1618.
11. Shaheen, R., Abdel-Salam, G.M., Guy, M.P., Alomar, R., Abdel-Hamid, M.S., Afifi, H.H., Ismail, S.I., Emam, B.A., Phizicky, E.M. and Alkuraya, F.S. (2015) Mutation in WDR4 impairs tRNA m(7)G46 methylation and causes a distinct form of microcephalic primordial dwarfism. *Genome Biol.*, **16**, 210.
12. Song, B., Tang, Y., Chen, K., Wei, Z., Rong, R., Lu, Z., Su, J., de Magalhaes, J.P., Rigden, D.J. and Meng, J. (2020) m7GHub: deciphering the location, regulation and pathogenesis of internal mRNA N7-methylguanosine (m7G) sites in human. *Bioinformatics*, **36**, 3528–3536.
13. Zhang, L.S., Liu, C., Ma, H., Dai, Q., Sun, H.L., Luo, G., Zhang, Z., Zhang, L., Hu, L., Dong, X., et al. (2019) Transcriptome-wide mapping of internal N(7)-methylguanosine methylome in mammalian mRNA. *Mol. Cell*, **74**, 1304–1316.
14. Li, W., Li, X., Ma, X., Xiao, W. and Zhang, J. (2022) Mapping the m1A, m5C, m6A and m7G methylation atlas in zebrafish brain under hypoxic conditions by MeRIP-seq. *BMC Genomics*, **23**, 105.
15. Wang, H., Chen, R.B., Zhang, S.N. and Zhang, R.F. (2022) N7-methylguanosine modification of lncRNAs in a rat model of hypoxic pulmonary hypertension: a comprehensive analysis. *BMC Genomics*, **23**, 33.
16. Zhang, B., Li, D. and Wang, R. (2022) Transcriptome profiling of N7-methylguanosine modification of messenger RNA in drug-resistant acute myeloid leukemia. *Front. Oncol.*, **12**, 926296.
17. Malbec, L., Zhang, T., Chen, Y.S., Zhang, Y., Sun, B.F., Shi, B.Y., Zhao, Y.L., Yang, Y. and Yang, Y.G. (2019) Dynamic methylome of internal mRNA N(7)-methylguanosine and its regulatory role in translation. *Cell Res.*, **29**, 927–941.
18. Enroth, C., Poulsen, L.D., Iversen, S., Kirpekar, F., Albrechtsen, A. and Vinther, J. (2019) Detection of internal N7-methylguanosine (m7G) RNA modifications by mutational profiling sequencing. *Nucleic Acids Res.*, **47**, e126.
19. Galalde, D.R., Snell, E.A., Jachimowicz, D., Sipos, B., Lloyd, J.H., Bruce, M., Pantic, N., Admassu, T., James, P., Warland, A., et al. (2018) Highly parallel direct RNA sequencing on an array of nanopores. *Nat. Methods*, **15**, 201–206.
20. Hendra, C., Pratanwanich, P.N., Wan, Y.K., Goh, W.S.S., Thiery, A. and Goke, J. (2022) Detection of m6A from direct RNA sequencing using a multiple instance learning framework. *Nat. Methods*, **19**, 1590–1598.
21. Lorenz, D.A., Sathe, S., Einstein, J.M. and Yeo, G.W. (2020) Direct RNA sequencing enables m(6)A detection in endogenous transcript isoforms at base-specific resolution. *RNA*, **26**, 19–28.
22. Huang, S., Zhang, W., Katanski, C.D., Dersh, D., Dai, Q., Lolans, K., Yewdell, J., Eren, A.M. and Pan, T. (2021) Interferon inducible pseudouridine modification in human mRNA by quantitative nanopore profiling. *Genome Biol.*, **22**, 330.
23. Jenjaroenpun, P., Wongsurawat, T., Wadley, T.D., Wassenaar, T.M., Liu, J., Dai, Q., Wanchai, V., Akel, N.S., Jamshidi-Parsian, A., Franco, A.T., et al. (2021) Decoding the epitranscriptional landscape from native RNA sequences. *Nucleic Acids Res.*, **49**, e7.
24. Boccaletto, P., Machnicka, M.A., Purta, E., Piatkowski, P., Baginski, B., Wirecki, T.K., de Crecy-Lagard, V., Ross, R., Limbach, P.A., Kotter, A., et al. (2018) MODOMICS: a database of RNA modification pathways. 2017 update. *Nucleic Acids Res.*, **46**, D303–D307.
25. Xuan, J.J., Sun, W.J., Lin, P.H., Zhou, K.R., Liu, S., Zheng, L.L., Qu, L.H. and Yang, J.H. (2018) RMBase v2.0: deciphering the map of RNA modifications from epitranscriptome sequencing data. *Nucleic Acids Res.*, **46**, D327–D334.
26. Luo, X., Li, H., Liang, J., Zhao, Q., Xie, Y., Ren, J. and Zuo, Z. (2021) RMVar: an updated database of functional variants involved in RNA modifications. *Nucleic Acids Res.*, **49**, D1405–D1412.
27. Bao, X., Zhang, Y., Li, H., Teng, Y., Ma, L., Chen, Z., Luo, X., Zheng, J., Zhao, A., Ren, J., et al. (2023) RM2Target: a comprehensive database for targets of writers, erasers and readers of RNA modifications. *Nucleic Acids Res.*, **51**, D269–D279.
28. Tang, Y., Chen, K., Song, B., Ma, J., Wu, X., Xu, Q., Wei, Z., Su, J., Liu, G., Rong, R., et al. (2021) m6A-Atlas: a comprehensive knowledgebase for unraveling the N6-methyladenosine (m6A) epitranscriptome. *Nucleic Acids Res.*, **49**, D134–D143.
29. Song, B., Chen, K., Tang, Y., Wei, Z., Su, J., de Magalhaes, J.P., Rigden, D.J. and Meng, J. (2021) ConsRM: collection and large-scale prediction of the evolutionarily conserved RNA methylation sites, with implications for the functional epitranscriptome. *Brief Bioinform.*, **22**, bbab088.
30. Sayers, E.W., Bolton, E.E., Brister, J.R., Canese, K., Chan, J., Comeau, D.C., Farrell, C.M., Feldgarden, M., Fine, A.M., Funk, K., et al. (2023) Database resources of the national center for biotechnology information in 2023. *Nucleic Acids Res.*, **51**, D29–D38.
31. Kim, D., Paggi, J.M., Park, C., Bennett, C. and Salzberg, S.L. (2019) Graph-based genome alignment and genotyping with HISAT2 and HISAT-genotype. *Nat. Biotechnol.*, **37**, 907–915.
32. Meng, J., Lu, Z., Liu, H., Zhang, L., Zhang, S., Chen, Y., Rao, M.K. and Huang, Y. (2014) A protocol for RNA methylation differential analysis with MeRIP-Seq data and exomePeak R/Bioconductor package. *Methods*, **69**, 274–281.
33. Huang, D., Song, B., Wei, J., Su, J., Coenen, F. and Meng, J. (2021) Weakly supervised learning of RNA modifications from low-resolution epitranscriptome data. *Bioinformatics*, **37**, i222–i230.
34. Sherry, S.T., Ward, M.-H., Kholodov, M., Baker, J., Phan, L., Smigielski, E.M. and Sirotkin, K. (2001) dbSNP: the NCBI database of genetic variation. *Nucleic Acids Res.*, **29**, 308–311.
35. Cunningham, F., Allen, J.E., Allen, J., Alvarez-Jarreta, J., Amode, M.R., Armean, I.M., Austine-Orimoloye, O., Azov, A.G., Barnes, J., Bennett, R., et al. (2022) Ensembl 2022. *Nucleic Acids Res.*, **50**, D988–D995.
36. Tomczak, K., Czerwińska, P. and Wiznerowicz, M. (2015) The Cancer Genome Atlas (TCGA): an immeasurable source of knowledge. *Contemporary Oncology*, **19**, A68.
37. Song, B., Wang, X., Liang, Z., Ma, J., Huang, D., Wang, Y., de Magalhaes, J.P., Rigden, D.J., Meng, J., Liu, G., et al. (2023) RMDisease V2.0: an updated database of genetic variants that affect RNA modifications with disease and trait implication. *Nucleic Acids Res.*, **51**, D1388–D1396.
38. Lorenz, R., Bernhart, S.H., Honer Zu Siederdisen, C., Tafer, H., Flamm, C., Stadler, P.F. and Hofacker, I.L. (2011) ViennaRNA Package 2.0. *Algorithms Mol Biol*, **6**, 26.
39. Zhu, Y., Xu, G., Yang, Y.T., Xu, Z., Chen, X., Shi, B., Xie, D., Lu, Z.J. and Wang, P. (2019) POSTAR2: deciphering the

- post-transcriptional regulatory logics. *Nucleic Acids Res.*, **47**, D203–D211.
40. Agarwal,V, Bell,G.W., Nam,J.-W. and Bartel,D.P. (2015) Predicting effective microRNA target sites in mammalian mRNAs. *eLife*, **4**, e05005.
 41. Li,J.-H., Liu,S., Zhou,H., Qu,L.-H. and Yang,J.-H. (2013) starBase v2.0: decoding miRNA-ceRNA, miRNA-ncRNA and protein–RNA interaction networks from large-scale CLIP-Seq data. *Nucleic Acids Res.*, **42**, D92–D97.
 42. Nassar,L.R., Barber,G.P., Benet-Pages,A., Casper,J., Clawson,H., Diekhans,M., Fischer,C., Gonzalez,J.N., Hinrichs,A.S., Lee,B.T., *et al.* (2023) The UCSC genome browser database: 2023 update. *Nucleic Acids Res.*, **51**, D1188–D1195.
 43. Kumar,P., Henikoff,S. and Ng,P.C. (2009) Predicting the effects of coding non-synonymous variants on protein function using the SIFT algorithm. *Nat. Protoc.*, **4**, 1073–1081.
 44. Adzhubei,I.A., Schmidt,S., Peshkin,L., Ramensky,V.E., Gerasimova,A., Bork,P., Kondrashov,A.S. and Sunyaev,S.R. (2010) A method and server for predicting damaging missense mutations. *Nat. Methods*, **7**, 248–249.
 45. Chun,S. and Fay,J.C. (2009) Identification of deleterious mutations within three human genomes. *Genome Res.*, **19**, 1553–1561.
 46. Shihab,H.A., Gough,J., Cooper,D.N., Stenson,P.D., Barker,G.L., Edwards,K.J., Day,I.N. and Gaunt,T.R. (2013) Predicting the functional, molecular, and phenotypic consequences of amino acid substitutions using hidden Markov models. *Hum. Mutat.*, **34**, 57–65.
 47. Wang,K., Li,M. and Hakonarson,H. (2010) ANNOVAR: functional annotation of genetic variants from high-throughput sequencing data. *Nucleic Acids Res.*, **38**, e164–e164.
 48. Landrum,M.J., Lee,J.M., Benson,M., Brown,G., Chao,C., Chitipiralla,S., Gu,B., Hart,J., Hoffman,D., Hoover,J., *et al.* (2015) ClinVar: public archive of interpretations of clinically relevant variants. *Nucleic Acids Res.*, **44**, D862–D868.
 49. Buniello,A., MacArthur,J.A.L., Cerezo,M., Harris,L.W., Hayhurst,J., Malangone,C., McMahon,A., Morales,J., Mountjoy,E., Sollis,E., *et al.* (2018) The NHGRI-EBI GWAS Catalog of published genome-wide association studies, targeted arrays and summary statistics 2019. *Nucleic Acids Res.*, **47**, D1005–D1012.
 50. Johnson,A.D. and O'Donnell,C.J. (2009) An open access database of genome-wide association results. *BMC Med. Genet.*, **10**, 6.
 51. Chang,C.C., Chow,C.C., Tellier,L.C., Vattikuti,S., Purcell,S.M. and Lee,J.J. (2015) Second-generation PLINK: rising to the challenge of larger and richer datasets. *Gigascience*, **4**, 7.
 52. Buels,R., Yao,E., Diesh,C.M., Hayes,R.D., Munoz-Torres,M., Helt,G., Goodstein,D.M., Elisk,C.G., Lewis,S.E., Stein,L., *et al.* (2016) JBrowse: a dynamic web platform for genome visualization and analysis. *Genome Biol.*, **17**, 66.
 53. Zhang,Y., Jiang,J., Ma,J., Wei,Z., Wang,Y., Song,B., Meng,J., Jia,G., de Magalhaes,J.P., Rigden,D.J., *et al.* (2023) DirectRMDDB: a database of post-transcriptional RNA modifications unveiled from direct RNA sequencing technology. *Nucleic Acids Res.*, **51**, D106–D116.